THE JOURNAL OF BIOLOGICAL CHEMISTRY VOL. 285, NO. 12, pp. 9114–9123, March 19, 2010

Critical Role of Flanking Residues in NGR-to-*iso*DGR Transition and CD13/Integrin Receptor Switching*[S]

Received for publication, July 14, 2009, and in revised form, December 30, 2009 Published, JBC Papers in Press, January 11, 2010, DOI 10.1074/jbc.M109.044297

Flavio Curnis[‡], Angela Cattaneo[‡], Renato Longhi[§], Angelina Sacchi[‡], Anna Maria Gasparri[‡], Fabio Pastorino[¶1], Paola Di Matteo[‖], Catia Traversari[‖], Angela Bachi[‡], Mirco Ponzoni[¶], Gian-Paolo Rizzardi[‖], and Angelo Corti[‡2]

From the [‡]Division of Molecular Oncology and IIT Network Research Unit of Molecular Neuroscience, San Raffaele Scientific Institute, 20132 Milan, the [§]Istituto di Chimica del Riconoscimento Molecolare, CNR, 20131 Milan, the [¶]Laboratory of Oncology, G. Gaslini Children's Hospital, 16148 Genoa, and [‖]MolMed SpA, 20132 Milan, Italy

Various NGR-containing peptides have been exploited for targeted delivery of drugs to CD13-positive tumor neovasculature. Recent studies have shown that compounds containing this motif can rapidly deamidate and generate isoaspartate-glycine-arginine (*iso*DGR), a ligand of αvβ3-integrin that can be also exploited for drug delivery to tumors. We have investigated the role of NGR and *iso*DGR peptide scaffolds on their biochemical and biological properties. Peptides containing the cyclic CNGRC sequence could bind CD13-positive endothelial cells more efficiently than those containing linear GNGRG. Peptide degradation studies showed that cyclic peptides mostly undergo NGR-to-*iso*DGR transition and CD13/integrin switching, whereas linear peptides mainly undergo degradation reactions involving the α-amino group, which generate non-functional six/seven-membered ring compounds, unable to bind αvβ3, and small amount of *iso*DGR. Structure-activity studies showed that cyclic *iso*DGR could bind αvβ3 with an affinity >100-fold higher than that of linear *iso*DGR and inhibited endothelial cell adhesion and tumor growth more efficiently. Cyclic *iso*DGR could also bind other integrins (αvβ5, αvβ6, αvβ8, and α5β1), although with 10–100-fold lower affinity. Peptide linearization caused loss of affinity for all integrins and loss of specificity, whereas α-amino group acetylation increased the affinity for all tested integrins, but caused loss of specificity. These results highlight the critical role of molecular scaffold on the biological properties of NGR/*iso*DGR peptides. These findings may have important implications for the design and development of anticancer drugs or tumor neovasculature-imaging compounds, and for the potential function of different NGR/*iso*DGR sites in natural proteins.

Various peptides containing the Asn-Gly-Arg (NGR) motif have been discovered by peptide-phage library panning in tumor-bearing mice (1). The tumor-homing properties of these peptides rely on the interaction with aminopeptidase N (CD13), a membrane protease expressed by the tumor neovasculature (2, 3). Because of this property, these peptides have been exploited for ligand-directed delivery of various drugs and particles to tumor vessels, in the attempt to increase their antitumor activity (4). For instance, we have shown that peptides containing cyclic CNGRC and linear GNGRG motives can be used for delivering tumor necrosis factor α (TNF)[3] (5–7), interferon γ (8–10), and liposomal doxorubicin (11, 12) to tumor neovasculature, improving their therapeutic properties. The CNGRC-TNF conjugate, called NGR-TNF, is currently tested in phase II clinical studies (13–15). Other investigators have used the NGR motif embedded in similar or different molecular scaffolds for delivering chemotherapeutic drugs, antiangiogenic drugs, tissue factor, viruses, and other compounds to tumor vessels (1, 16–32). Recently, a CNGRC peptide with an acetylated N-terminal α-amino group has been successfully exploited also for quantitative molecular magnetic resonance imaging of tumor angiogenesis using peptide-labeled paramagnetic quantum dots (30).

Although it is generally assumed that all these NGR compounds bind CD13 on tumor neovasculature, the role of different molecular scaffolds on peptide binding properties remains to be clarified.

Recent studies showed that the Asn residue of NGR can rapidly deamidate and generate Asp and *iso*Asp residues (33). This spontaneous reaction occurs by nucleophilic attack of the backbone NH center on the Asn side chain leading to formation of a succinimide intermediate (34). Hydrolysis of succinimide leads, in turn, to formation of mixtures of *iso*DGR and DGR, with changes in charge and peptide bond length (33). The transition of NGR to *iso*DGR/DGR is associated with loss of CD13 binding and gain of αvβ3-integrin binding activity (33). Biochemical studies, NMR structure analysis and αvβ3 docking experiments showed that *iso*DGR, but not NGR and DGR, can fit into the RGD-binding pocket of this integrin, recapitulating not only the canonical RGD/αvβ3 contacts but also establishing additional polar interactions (33, 35). Because of increased expression of αvβ3 integrin in tumor neovasculature, *iso*DGR has been exploited for ligand-directed delivery of TNF to tumors (36), suggesting that peptides containing this motif may represent a new class of ligands for the tumor vasculature.

* This work was supported in part by the Associazione Italiana per la Ricerca sul Cancro (AIRC) and Alleanza Contro il Cancro (ISS).

[S] The on-line version of this article (available at http://www.jbc.org) contains supplemental Fig. S1 and Tables S1 and S2.

[1] A "Fondazione Italiana per la Lotta al Neuroblastoma" research fellow.

[2] To whom correspondence should be addressed: Division of Molecular Oncology, San Raffaele Scientific Institute, via Olgettina 58, 20132 Milan, Italy. Tel.: 39-02-26434802; Fax: 39-02-26434786; E-mail: corti.angelo@hsr.it.

[3] The abbreviations used are: TNF, tumor necrosis factor; BSA, bovine serum albumin; PBS, phosphate-buffered saline; DAPI, 4′,6-diamidino-2-phenylindole; *iso*DGR, *iso*Asp-Gly-Arg; HRP, horseradish peroxidase.

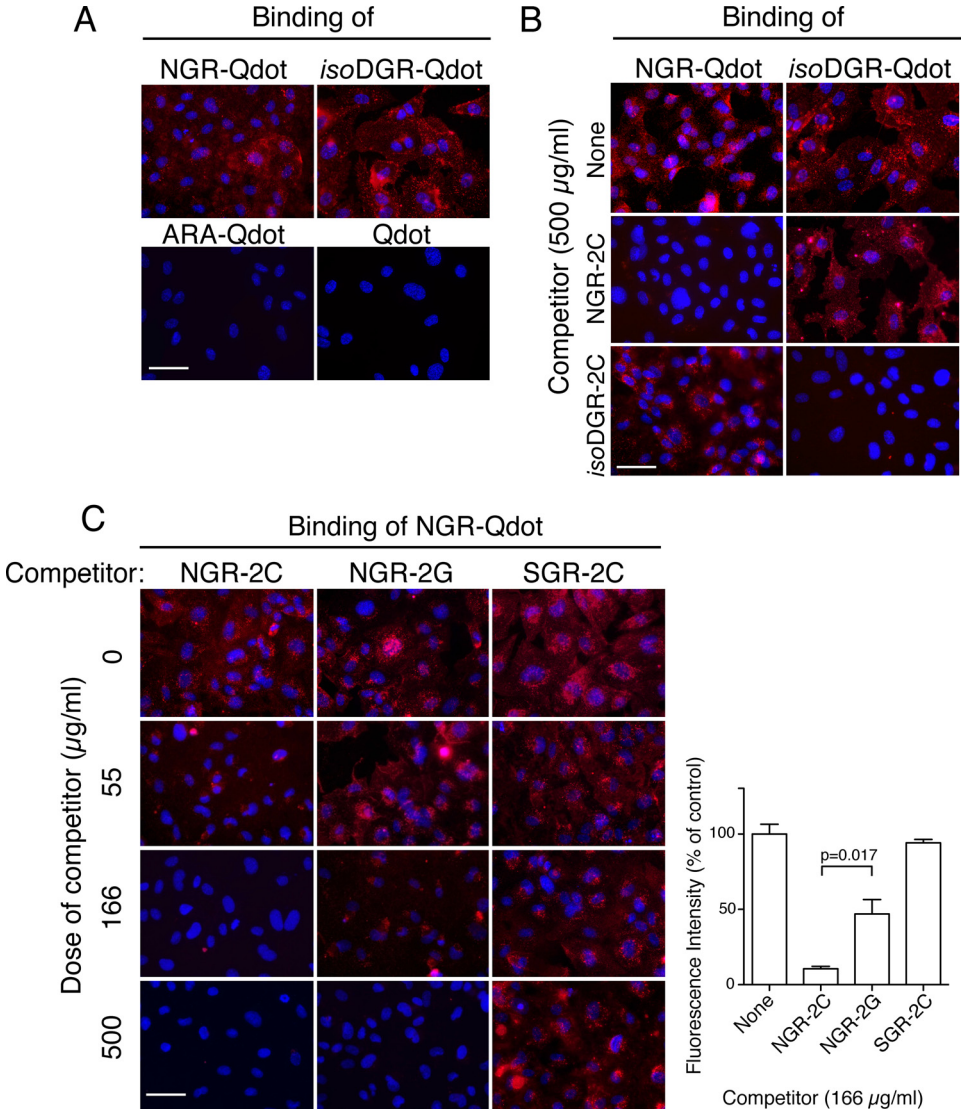

FIGURE 1. **Competitive binding of NGR-Qdot with cyclic and linear NGR peptides to HUVECs.** *A*, binding of NGR-Qdot, *iso*DGR-Qdot, ARA-Qdot, and Qdot (1:100) to HUVECs. *B*, competitive binding of NGR-Qdot and *iso*DGR-Qdot with NGR-2C and *iso*DGR-2C (500 μg/ml). *C*, competitive binding of NGR-Qdot with various doses of NGR-2C, NGR-2G or SGR-2C. Fluorescence microscopy assays were carried out as described under "Experimental Procedures." Representative images of three independent experiments are shown (*left*). Quantification of staining intensity was performed by using the CellF Software (Olympus Soft Imaging Solutions GmbH, Germany) (*right*). Four images were analyzed for each condition. Magnification, ×400; scale bar, 50 μm; *red*, Qdot; *blue*, nuclear staining with DAPI.

The role of flanking residues and molecular constraints on NGR deamidation reaction and on *iso*DGR integrin binding specificity is unknown. Remarkably, NGR deamidation can take place not only in peptides and peptide-drug conjugates, but also in fibronectin, an extracellular matrix protein that contains four NGR sites with different flanking residues (including two GNGRG sites) with important physiological implications (33, 37). Studies aimed at investigating the role of different molecular scaffolds on NGR/*iso*DGR biological properties and stability are, therefore, of great physiological and pharmacological interest.

In this work, we have investigated the role of NGR/*iso*DGR flanking residues and molecular constraints on the biochemical and functional properties of these tumor vasculature-targeting motives. We show that the molecular scaffold critically affects the transition of NGR to *iso*DGR as well as the generation of other non-functional derivatives. Furthermore, we show that the NGR/*iso*DGR flanking residues are critical for their receptor binding affinity/specificity and biological activity *in vitro* and *in vivo*.

EXPERIMENTAL PROCEDURES

Cell Lines and Reagents—Human umbilical vein endothelial cells (HUVECs) (Clonetics, Lonza, Switzerland) were cultured according to the recommended protocols. Human EA.hy926 endothelial cells and murine WEHI-164 fibrosarcoma cells were cultured as described (8). Human α5β1, αvβ3, and αvβ5 integrins were from Immunological Sciences (Rome, Italy), recombinant human αvβ6 and αvβ8 integrins were from R&D System (Minneapolis, MN). The following peptides were prepared as previously described (5, 6, 38): GNGRGGVRSSSRTPSDKY and CNGRCGVRSSSRTPSDKY (called NGR-2G-TNF$_{1-11}$ and NGR-2C-TNF$_{1-11}$, respectively), GNGRGGVRY (NGR-2G), CNGRCGVRY (NGR-2C), G*iso*DGRGGRVY (*iso*DGR-2G), C*iso*DGRCGRVY (*iso*DGR-2C). Similar peptides with acetyl groups linked to the α-amino group were also prepared (*ac-iso*DGR-2G and *ac-iso*DGR-2C). All peptides were dissolved in water and stored in aliquots at −20 °C. The molecular mass of each peptide was checked by MALDI-TOF mass spectrometry (MS) analysis. NGR-Qdot, ARA-Qdot, and *iso*DGR-Qdot conjugates (consisting of *ac*-NGR-2C-TNF$_{1-11}$, *ac*-ARA-2C-TNF$_{1-11}$ and *ac-iso*DGR-2C-TNF$_{1-11}$ chemically coupled to amine-modified quantum dots) were prepared as described (36).

NGR/STV-HRP, *iso*DGR/STV-HRP, and ARA/STV-HRP complexes (consisting of mixtures of biotinylated NGR-2C-TNF$_{1-11}$, *iso*DGR-2C-TNF$_{1-11}$ and ARA-2C-TNF$_{1-11}$ and streptavidin-peroxidase (STV-HRP) were prepared as described (35). *iso*DGR-TNF (consisting of murine TNF fused to the C terminus of C*iso*DGRCG) was prepared as described (36).

Peptide Stability Studies—Peptide stability and forced degradation studies were performed by incubating peptides in various buffers and temperature conditions. The product were then analyzed by reverse-phase HPLC (RP-HPLC) and MALDI-TOF MS. RP-HPLC was performed using a C18 column (PepMap C18, 250 × 4.6 mm, PerSeptive Biosystem, Framingham, MA)

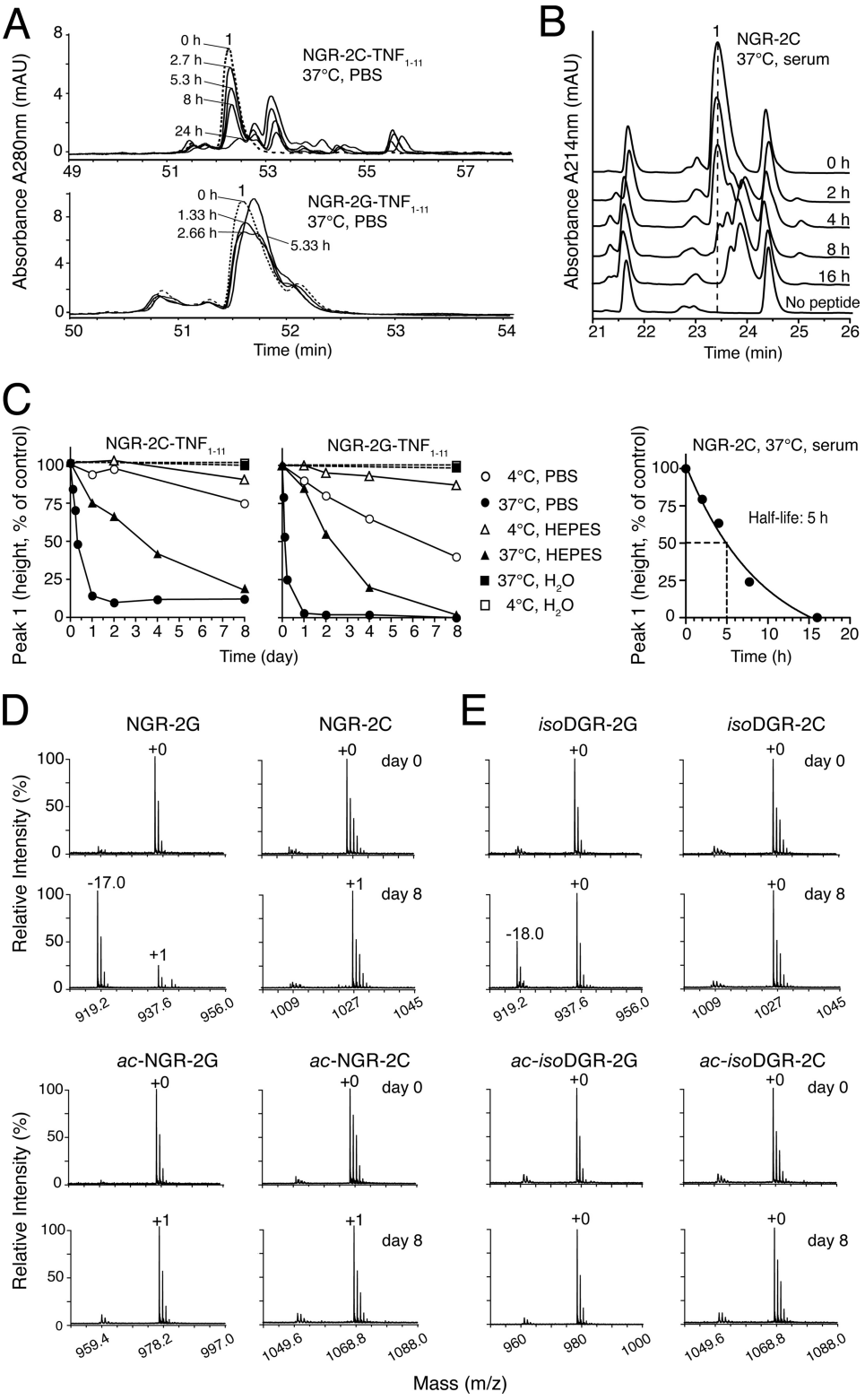

FIGURE 2. **Differential stability of cyclic and linear NGR and *iso*DGR peptides.** *A*, RP-HPLC of NGR-2C-TNF$_{1-11}$ (5 μg) and NGR-2G-TNF$_{1-11}$ (5 μg) after incubation at 37 °C in PBS. *Dotted line*, untreated peptide. Peak 1 corresponds to NGR-2C-TNF$_{1-11}$; peak height was proportional to the loaded material within the range of 1–50 μg. *B*, RP-HPLC of NGR-2C after incubation at 37 °C in human serum. The peptide was added to human serum (500 μg/ml, final concentration) and incubated for the indicated time. The sample was then ultrafiltered through a 5 kDa cut-off ultrafilter (Vivaspin 500, Sartorius, Italy). The permeate (50 μl) was analyzed by RP-HPLC. Peak 1 corresponds to NGR-2C. *C*, stability of NGR-2C-TNF$_{1-11}$, NGR-2G-TNF$_{1-11}$, and NGR-2C after incubation at 37 °C or at 4 °C in PBS, HEPES buffer, water, or human serum, as determined by RP-HPLC. *D* and *E*, MALDI-TOF MS analysis of non-acetylated and acetylated NGR-2G, NGR-2C, *iso*DGR-2G, and *iso*DGR-2C after incubation at 37 °C for 0 and 8 days in PBS. +0, +1, −17, and −18 correspond to the difference between the found and the expected molecular masses in daltons.

connected with a guard column (Wakosil C18RS 10 × 4.0 mm, SGE Analytical Science, Italy). Mobile phase A, 0.1% trifluoroacetic acid in water; mobile phase B, 95% acetonitrile, 0.1% trifluoroacetic acid; 0% B for 10 min, linear gradient 0–27.5% B in 55 min, 100% B for 10 min, 0% of B for 15 min (flow rate, 0.5 ml/min). Peptide elution was monitored by measuring the absorbance at 214 nm and 280 nm (HPLC, LC-126 nM, Beckman Coulter).

1-μl aliquots of samples (200 μg/ml), diluted 1:100 v/v with water, were analyzed by MS analysis using a MALDI-TOF Voyager-DE STR mass spectrometer (Applied Biosystems, Framingham, MA) (dried droplet technique and α-cyano-4-hydroxycinnamic acid as matrix). Spectra were accumulated over a mass range of 750–2000 Da with a mean resolution of about 15,000. Spectra were externally calibrated using matrix signals and trypsin autolysis peaks then processed via Data Explorer software version 4.0.0.0 (Applied Biosystems).

Competitive Binding Assays of NGR-Qdot/isoDGR-Qdot to HUVECs—Binding assays of NGR-Qdot and *iso*DGR-Qdot were carried out as follows: HUVEC cells were grown in chamber slides (5×10^4 cell/well, plated 48 h before the experiment). After washing with 25 mM HEPES buffer, pH 7.4, containing 150 mM sodium chloride, 1 mM magnesium chloride, 1 mM manganese chloride, 1% bovine serum albumin (BSA), and 0.1% sodium azide (called "Binding Buffer"), NGR-Qdot and *iso*DGR-Qdot (1:100, in Binding Buffer) were added to the cells and left to incubate for 2 h at room temperature. After washing with Binding Buffer, cells were fixed with 2% paraformaldehyde, 3% sucrose in 50 mM sodium phosphate buffer, pH 7.3, containing 150 mM (PBS) for 15 min at room temperature. DNA was counterstained with DAPI (Invitrogen), and cells were then analyzed using an Olympus BX61 microscope (excitation filter, E460SPUVv2; emission filter, D605/20m, Chroma Technology Corp, Rockingham,

VT). Competitive binding of NGR-Qdot and *iso*DGR-Qdot with NGR-2G, *iso*DGR-2G, *iso*DGR-2C or SGR-2C were performed as described above.

Competitive Binding Assay of isoDGR Peptides to Integrins—Competitive binding assays of linear and cyclic *iso*DGR-peptides to $\alpha v\beta 3$, $\alpha v\beta 5$, $\alpha v\beta 6$, $\alpha v\beta 8$, and $\alpha 5\beta 1$ integrins were performed as follows: the *ac-iso*DGR/STV-HRP complex was diluted with 25 mM Tris-HCl, pH 7.4, containing 150 mM sodium chloride, 1 mM magnesium chloride, 1 mM manganese chloride, and 3% BSA, and mixed with various amounts of *iso*DGR-2G or *iso*DGR-2C peptides (acetylated and non-acetylated). The mixtures were then added to microtiter plates coated with integrins and incubated for 2 h at room temperature. After washing, each well was incubated with 70 μl of 3,3′,5,5′-tetramethylbenzidine chromogenic solution (Sigma) for 20 min, at room temperature. The chromogenic reaction was stopped by adding an equal volume of 1 N sulfuric acid. The absorbance at 450 nm was then measured using a microtiter-plate reader.

Cell Adhesion Assay—Cell adhesion assays were carried out using 96-well polyvinyl chloride microtiter plates as described (33). Briefly, microtiter plates were coated with *iso*DGR-TNF (5 μg/ml in PBS, overnight at 4 °C). After washing with PBS the plates were incubated for 1 h with in Dulbecco's modified Eagle's medium (DMEM) containing 3% BSA and seeded with EA.hy926 cells mixed with various amounts of *iso*DGR-2G and *iso*DGR-2C peptides. Non-adherent cells were removed by washing the plate with DMEM. Adherent cells were fixed with 2% paraformaldehyde, 4% sucrose, in PBS for 10 min at room temperature. The cells were stained with 0.5% crystal violet solution (Fluka Chemie, Buchs, Switzerland) for 10 min and washed with 0.9% sodium chloride. Cell adhesion was then quantified by measuring the absorbance at 560 nm, using a microtiter plate reader.

In Vivo Studies—Studies on animal models were approved by the Ethical Committee of the San Raffaele Scientific Institute, Milan, and performed according to the prescribed guidelines. BALB/c (Charles River Laboratories, Calco, Italy), weighing 16–18 g were challenged with subcutaneous injection in the left flank of 10^6 WEHI-164 cells. Mice were then treated with *ac-iso*DGR-2G and *ac-iso*DGR-2C peptide (5 mg/kg in 100 μl of 0.9% sodium chloride, intraperitoneal, at day 5, 6, 7, 8, 9, and 12). Tumor growth was monitored daily by measuring tumor volumes with calipers, as described (39). Animals were sacrificed before tumor diameter reached 1.0–1.5 cm. Tumor size is shown as percentage increase of tumor volume after treatment (mean ± S.E.) of three independent experiments (5–6 mice/group in each experiment).

RESULTS

NGR and isoDGR Peptides Bind Distinct Receptors on Cultured Endothelial Cells—Previous studies have provided evidence to suggest that NGR and *iso*DGR can bind CD13 and $\alpha v\beta 3$, respectively, on endothelial cells (2, 3, 5, 33). We have coupled cyclic peptides containing the NGR, *iso*DGR and ARA motives to Qdot-fluorescent nanoparticles and studied their binding to HUVEC, a primary endothelial cell line that express both CD13 and $\alpha v\beta 3$ integrin. Fluorescence microscopy experiments showed that NGR-Qdot, *iso*DGR-Qdot, but not the ARA-Qdot (negative control) can bind to HUVECs (Fig. 1*A*). The binding of NGR-Qdot was completely inhibited by an excess of CNGRCGVRY peptide (NGR-2C), but not by C*iso*DGRCGVRY (*iso*DGR-2C), while *iso*DGR-Qdot staining was completely inhibited by *iso*DGR-2C, but not by NGR-2C (Fig. 1*B*). These results are in line with the concept that NGR and *iso*DGR can bind different receptors on the surface of endothelial cells.

TABLE 1
Quantification of functional *iso*DGR in cyclic and linear NGR peptides before and after forced degradation (37 °C in PBS) as measured by competitive $\alpha v\beta 3$ integrin binding assay

Peptide	Storage	*iso*DGR[a]
	days	*%*
*iso*DGR-2C	0	100
NGR-2C	0	<1
	8	72 ± 9
*ac-iso*DGR-2C	0	100
ac-NGR-2C	0	2 ± 1
	8	61 ± 12
*iso*DGR-2G	0	100
NGR-2G	0	3 ± 1
	8	17 ± 6
*ac-iso*DGR-2G	0	100
ac-NGR-2G	0	3 ± 1
	8	62 ± 3

[a] The *iso*DGR content in NGR peptides was quantified using the corresponding *iso*DGR peptides as reference standards.

We have also performed immunofluorescence co-staining experiments of NGR-Qdot and *iso*DGR-Qdot with anti-CD13 mAb WM15 and anti-$\alpha v\beta 3$ mAb LM609, respectively. The results show that there is good overlapping between antibody and peptide-Qdot staining (supplemental Fig. S1). Of note, some areas stained by the anti-$\alpha v\beta 3$ antibody were not stained by *iso*DGR-Qdot, suggesting that $\alpha v\beta 3$ exists in active and inactive conformations.

NGR Flanking Residues Affect Binding to Endothelial Cells—We then analyzed the capability of linear GNGRGGVRY (NGR-2G) and cyclic NGR-2C to compete the binding of NGR-Qdot to HUVECs. We found that NGR-2C inhibits the binding of NGR-Qdot about 3-fold more efficiently than NGR-2G (Fig. 1*C*). No inhibition of NGR-Qdot was observed with SGR-2C, a control peptide. These results suggest that linear and cyclic peptides bind endothelial cells with different affinity.

NGR Flanking Residues Affect Peptide Stability—Next we investigated the role of molecular scaffold on NGR peptide stability. To this aim we compared the stability of CNGRCGVRSSSRTPSDKY (NGR-2C-TNF_{1-11}) with that of linear GNGRGGVRSSSRTPSDKY (NGR-2G-TNF_{1-11}), *i.e.* two peptides currently used for targeted delivery of TNF and liposomes to tumors (5, 11). These peptides were analyzed by RP-HPLC before and after incubation in PBS (pH 7.3), HEPES (pH 7.4), or water, at 37 °C or 4 °C. The half-lives of NGR-2C-TNF_{1-11} and NGR-2G-TNF_{1-11} (at 37 °C) were 6–8 h and 3–4 h, respectively, in PBS, and 2 days and 3.5 days, respectively, in HEPES buffer (Fig. 2, *A* and *C*). Of note, no major changes were observed with both peptides after incubation in water at 37 °C or 4 °C for more than 1 week. Both peptides were stable for more than 3 years when stored in water at −20 °C or in a lyophilized formulation at 4 °C (data not shown). The stability of NGR-2C and NGR-2G in serum was also evaluated. The half-

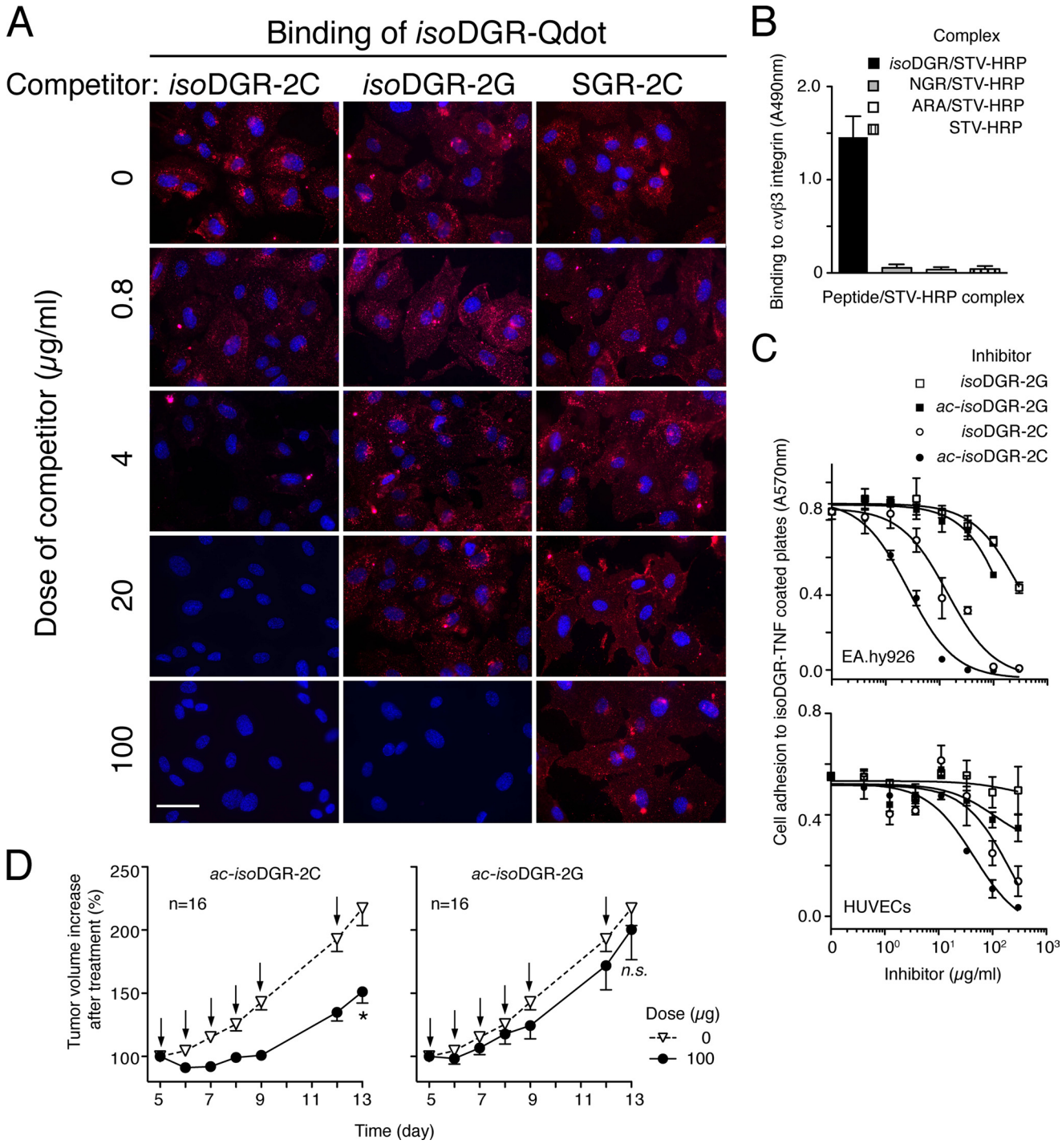

FIGURE 3. **Functional properties of different *iso*DGR peptides: αvβ3 integrin binding, inhibition of endothelial cell adhesion, and inhibition of tumor growth.** *A*, competitive binding of *iso*DGR-Qdot with various doses of *iso*DGR-2C, *iso*DGR-2G, or SGR-2C to HUVECs. Representative images of three independent experiments are shown. Fluorescence microscopy assays were carried out as described under "Experimental Procedures." Magnification, ×400; scale bar, 50 μm; *red*, Qdot; *blue*, nuclear staining with DAPI. *B*, binding of NGR/STV-HRP, *iso*DGR/STV-HRP, and ARA/STV-HRP to αvβ3 integrin. Complexes were diluted 1:500 in 25 mM Tris-HCl, pH 7.4, containing 150 mM sodium chloride, 1 mM magnesium chloride, 1 mM manganese chloride, 3% BSA (1:500), added to microtiter plates coated with αvβ3, and incubated for 2 h at room temperature. After washing, the binding was detected by chromogenic reaction with 3,3′,5,5′-tetramethylbenzidine chromogenic substrate. Mean ± S.E. of three independent experiments (each in duplicate). *C*, inhibition of EA.hy926 cells adhesion (*upper panel*) or HUVECs adhesion (*lower panel*) to *iso*DGR-TNF-coated plates by acetylated (*ac*) and non-acetylated *iso*DGR-2C and *iso*DGR-2G peptides. Cell adhesion assay was performed as described under "Experimental Procedures." The representative results of three independent experiments (each in duplicate) is shown. *D*, anti-tumor effect of repeated administrations of *ac-iso*DGR-2C or *ac-iso*DGR-2G peptide (5 mg/kg, intraperitoneal) to WEHI-164 tumor-bearing mice. Animals were treated at the indicated times (*arrows*). Cumulative data of three independent experiments (16 mice/group in total) (mean ± S.E.) are shown. Two-tailed *t* test at day 13: *, $p < 0.0003$; *n.s.*, not significant.

life of NGR-2C at 37 °C was 5 h (Fig. 2, *B* and *C*), whereas that of NGR-2G was about 3 h (not shown). These results indicate that peptide stability strongly depends on buffer composition and temperature as well as on the presence or absence of molecular constraints. However, it is remarkable that both linear and cyclic peptides are very stable in water.

TABLE 2
Binding of linear and cyclic *iso*DGR peptides (acetylated and not acetylated) to integrins as measured by competitive binding assay

Competitor	Binding of ac-*iso*DGR/STV-HRP to									
	αvβ3		αvβ5		αvβ6		αvβ8		α5β1	
	n^a	K_i^b	*n*	K_i	*n*	K_i	*n*	K_i	*n*	K_i
		nM		nM		nM		nM		nM
*iso*DGR-2C	6	9 ± 2	6	380 ± 108	6	118 ± 39	4	710 ± 68	*4*	95 ± 33[f]
*ac-iso*DGR-2C	5	2 ± 0.4[c]	5	29 ± 7	4	5 ± 2	3	22 ± 6	*3*	6 ± 2
*iso*DGR-2G	3	1086 ± 186[d]	3	6138 ± 1756	3	256 ± 52	3	7370 ± 820	*3*	1489 ± 424
*ac-iso*DGR-2G	3	254 ± 81[e]	3	845 ± 65	3	163 ± 26	3	878 ± 71	*3*	226 ± 39

[a] *n*, number of independent experiments (each in duplicate).
[b] K_i: equilibrium dissociation constant of the competitor (mean ± S.E.). K_i was calculated by nonlinear regression analysis of competitive binding data by using the "One site-Fit K_i" equation of the GraphPad Prism Software (GraphPad Software, Version 5.00 San Diego, CA).
[c] $p < 0.05$ (ac-*iso*DGR-2C versus *iso*DGR-2C).
[d] $p < 0.05$ (*iso*DGR-2G versus *iso*DGR-2C).
[e] $p < 0.01$ (ac-*iso*DGR-2G versus ac-*iso*DGR-2C).
[f] $p < 0.05$ (α5β1 versus αvβ3).

Linear and Disulfide-constrained NGR Peptides Generate Different Degradation Products—The Asn residue of CNGRC can deamidate via succinimide formation and loss of ammonia (−17 Da), followed by rapid hydrolysis and formation of Asp and *iso*Asp, with an overall gain of 1 Da (33). It is also known that peptides containing Asn in the second position may undergo additional intramolecular reactions involving the N-terminal α-amino group, loss of ammonia (−17 Da), and formation of six/seven-membered rings (40, 41). To characterize the structural changes occurring in linear and cyclic peptides after degradation, we monitored peptide degradation by MALDI-TOF MS. Storage of cyclic NGR-2C-TNF_{1-11} at 37 °C for 8 days in PBS generated a large amount of a product characterized by a gain of 1 Da (+1 Da product), likely corresponding to a DGR/*iso*DGR mixture. Conversely, storage of linear NGR-2G-TNF_{1-11} under the same conditions generated a product characterized by loss of 17 Da (−17 Da product) and only small amounts of the +1 Da product (supplemental Table S1). We observed similar degradation patterns also with shorter peptides (NGR-2C and NGR-2G) after incubation for 1 day or 8 days (Fig. 2*D*, *upper panel* and supplemental Table S1). To assess whether the −17 Da degradation product described above was related to the succinimide intermediate of Asn deamidation and/or to other reaction involving the N-terminal α-amino group (leading to the formation of six/seven-membered ring compounds), we performed forced degradation studies of linear and cyclic peptides with acetylated α-amino group. Acetylation of NGR-2G markedly decreased the formation of the −17 Da product both in PBS and in HEPES (Fig. 2*D*, *lower panels* and supplemental Table S2), pointing out the crucial role of α-amino group in peptide degradation. Because succinimide formation does not involve the α-amino group, these results provide support for the hypothesis that the −17 Da product corresponds to six/seven-membered ring compounds. Consistently, blockade of the α-amino group in the linear peptide apparently enhanced Asn deamidation, as suggested by the increased production of the +1 Da product following incubation in PBS for 8 days (Fig. 2*D*, *lower panel*). Of note, the −17 Da degradation product was apparently stable even after incubation for 8 days at 37 °C (supplemental Table S1).

In conclusion, the results of peptide degradation studies suggest that linear NGR mainly generates a −17 Da degradation product, likely corresponding to six/seven membered ring compounds, whereas cyclic NGR mainly generates a +1 Da product, likely corresponding to *iso*DGR/DGR. Thus, the NGR molecular scaffold markedly affects the peptide degradation pattern.

The Main Degradation Products of NGR-2C, but Not of NGR-2G, Bind αvβ3 Integrin—We have previously shown that *iso*DGR can efficiently bind to αvβ3 integrin (36). To investigate the functional properties of the degradation products of linear and cyclic NGR peptides, we then analyzed the capability of NGR-2C-and NGR-2G-forced degradation products to compete the binding of an *iso*DGR peptide in a competitive αvβ3 integrin binding assay (33). We found that 72 ± 9% of NGR-2C molecules could generate functional molecules in these conditions (Table 1). Considering that Asn deamidation is expected to generate *iso*DGR/DGR mixtures in a 3:1 ratio and that DGR cannot bind αvβ3 (35), this result suggests that most NGR-2C molecules can undergo deamidation, generating biologically active *iso*DGR. Conversely, only 17 ± 6% of NGR-2G generated bioactive *iso*DGR, despite the peptide was totally degraded in these conditions. This implies that the main degradation product of linear peptides (*i.e.* the −17 Da product) is non-functional. Noteworthy, acetylation of the N-terminal α-amino group of NGR-2G, which inhibits the formation of the −17 Da product, increased the percentage of functional *iso*DGR to 62 ± 3%, after forced degradation. This confirms the hypothesis that acetylation of the linear peptide markedly change its degradation pattern, from inactive six/seven-membered ring derivatives to active *iso*DGR.

isoDGR Flanking Residues Affect Peptide Stability and Binding to Endothelial Cells—Considering that *iso*DGR may represent not only a potential degradation product of certain NGR drugs conjugates, but also a novel tumor vasculature ligand for targeted delivery of drugs to tumors and an efficient antagonist of RGD/αvβ3 interactions (33, 36), we next studied the role of *iso*DGR flanking residues on peptide stability and endothelial cell binding. Adopting a similar strategy to that described for NGR peptides, we synthesized linear G*iso*DGRGGVRY (*iso*DGR-2G) and cyclic *iso*DGR-2C, and verified the impact of different scaffolds on peptide stability following forced degradation (8 days at 37 °C in PBS). We observed that *iso*DGR-2G is less stable than *iso*DGR-2C, as an 18-Da degradation product was observed only with the linear peptide (Fig. 2*E*, *upper panel*). Given that *iso*Asp can undergo

isomerization reactions via formation of the succinimide intermediate (34), it is likely that also in this case the α-amino group reacted with the succinimide ring, forming the six/seven-membered ring compounds, both characterized by loss of 18 Da. Accordingly, peptide acetylation blocked the formation of the 18 Da product (Fig. 2*E*, *lower panel*). We then analyzed the capability of linear *iso*DGR-2G and cyclic *iso*DGR-2C to compete the binding of *iso*DGR-Qdot to HUVECs. We found that *iso*DGR-2C competed the binding of *iso*DGR-Qdot 10–20-fold more efficiently than *iso*DGR-2G (Fig. 3*A*). These results suggest that linear and disulfide constrained peptides recognize endothelial cell membrane receptors with different affinity.

isoDGR Flanking Residues Affect the Binding Affinity and Specificity of isoDGR Peptides for Integrins—Binding studies with microtiter plates coated with integrins confirmed that cyclic *iso*DGR, but not NGR, can bind αvβ3 (Fig. 3*B*). No binding of *iso*DGR to α1β1, α3β1, α4β7 α6β4, or α9β1 integrins was observed (not shown). To provide more information on the affinity and selectivity of linear and cyclic *iso*DGR peptides for different integrins, we performed competitive binding experiments using microtiter plates coated with αvβ3, α5β1, αvβ5, αvβ6, and αvβ8. Each peptide, acetylated and non-acetylated, was tested in competitive binding assay using *ac-iso*DGR/STV-HRP conjugate as tracer (Table 2). We observed that 1) *iso*DGR-2C binds αvβ3 with an affinity 10–100-fold greater than that for other integrins; 2) the relative affinity of *iso*DGR-2C and *iso*DGR-2G for these integrins was different (αvβ3>α5β1≥αvβ6>αvβ5>αvβ8 and αvβ6>αvβ3>α5β1>αvβ5≥αvβ8, respectively); Ref. 3) acetylation of *iso*DGR-2C and *iso*DGR-2G increased the affinity for all integrins in a differential manner and caused loss of selectivity.

Of note, *iso*DGR-2C could bind αvβ3 with an affinity 10-fold greater

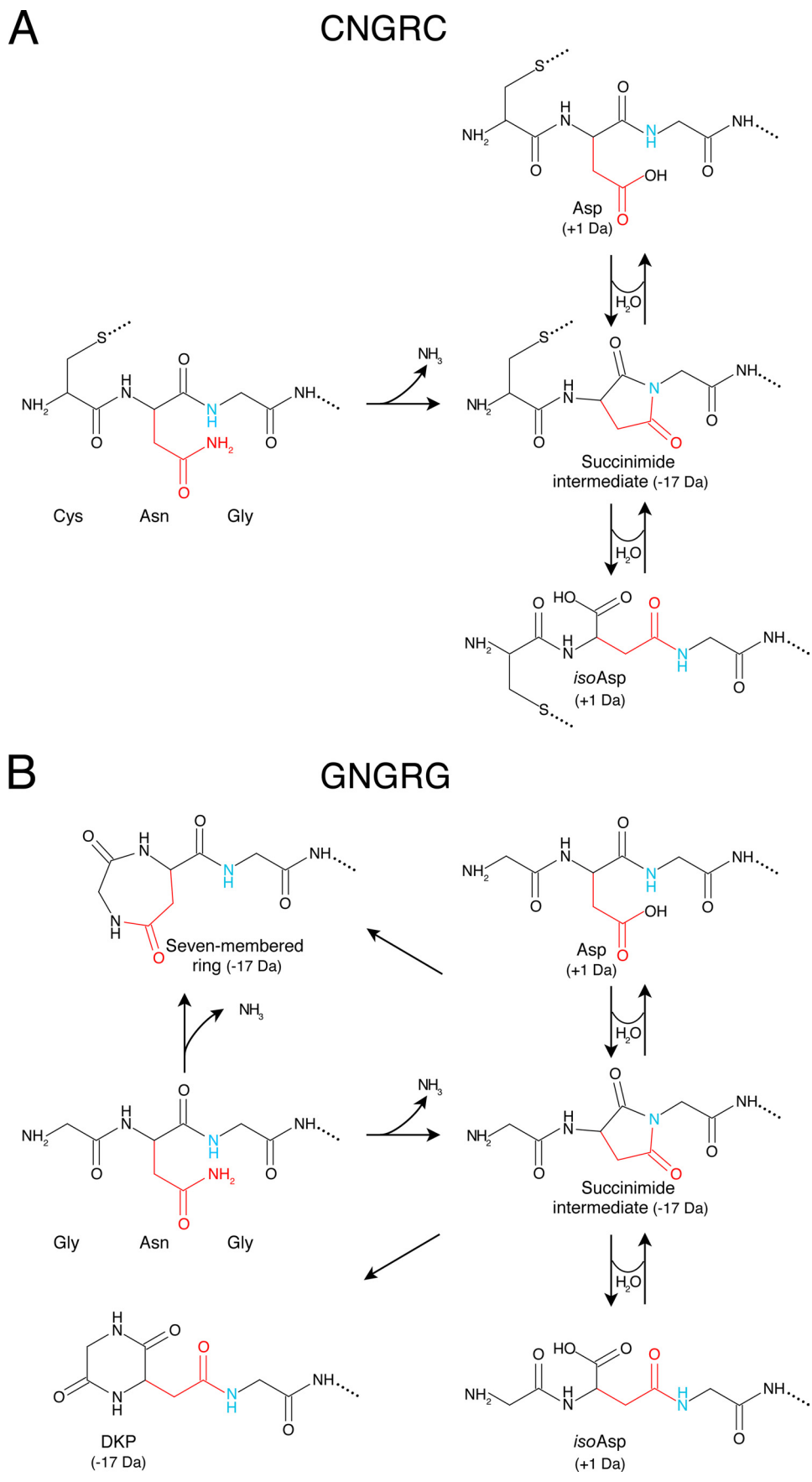

than that for $\alpha5\beta1$, whereas ac-*iso*DGR-2C, *iso*DGR-2G, and *ac-iso*DGR-2G could not discriminate between these integrins. Overall, these results suggest that changes in the molecular scaffold can significantly affect not only binding affinity, but also receptor selectivity.

Cyclic isoDGR Inhibits Endothelial Cell Adhesion and Tumor Growth More Efficiently than Linear isoDGR—The functional properties of cyclic and linear *iso*DGR peptides were then investigated *in vitro* and *in vivo*. We analyzed, first, the capability of these peptides to inhibit endothelial cell adhesion to microtiter plates. Both linear and cyclic *iso*DGR could inhibit EA.hy926 and HUVEC cell adhesion, although with different potency (Fig. 3*C*). Remarkably, peptide acetylation increased the potency of both *iso*DGR peptides on both cell lines. The stronger affinity of *ac-iso*DGR-2C for various integrins compared with that of the other peptides (Table 2) may explain its higher efficiency in these assays. Next we performed *in vivo* experiments. Previous studies have shown that $\alpha v\beta3$-binding peptides can inhibit tumor growth (33). We therefore analyzed the anti-tumor activity of acetylated linear and cyclic *iso*DGR peptides using WEHI-164-fibrosarcoma-bearing mice. *Ac-iso*DGR-2C delayed tumor growth more efficiently than *ac-iso*DGR-2G (Fig. 3*D*). The results of *in vitro* and *in vivo* experiments support the concept that changes in flanking residues critically affect the biological activity of *iso*DGR.

DISCUSSION

Various peptides containing the NGR motif embedded in different molecular scaffolds, such as CNGRC, acetylated-CNGRC, GNGRG, NGRAHA, CVLNGRMEC, are currently used by different investigators to deliver cytokines, chemotherapeutic drugs, liposomes, anti-angiogenic compounds, virus, imaging agents, and DNA complexes, to CD13-positive tumor neovasculature (4). These peptides have been chemically coupled to drugs and particles or fused to the N-terminal or C-terminal sequences of protein or even incorporated in internal loops by genetic engineering technology (1, 5, 6, 8, 11, 12, 16–31, 33). Although it is generally assumed that these peptides bind CD13 on tumor neovasculature, the role of different molecular scaffolds on binding affinity is unclear. The results of the present work indicate that (*a*) different molecular scaffolds may confer different biochemical and biological properties to the NGR motif, including binding to CD13-positive endothelial cells and peptide degradation, (*b*) one of the degradation pathway of NGR leads to the formation of *iso*DGR, which can bind to integrins, and (*c*) different molecular scaffolds of *iso*DGR may differentially affect the affinity for different integrins.

In particular, the results of binding studies showed that the affinity of cyclic CNGRC for CD13-positive endothelial cells is greater than that of linear GNGRG. Furthermore, forced-degradation studies showed that these NGR peptides can undergo differential degradation reactions: while the molecular mass of the main degradation product of cyclic NGR peptides is characterized by a gain of 1 Da, compared with the original peptide, the main degradation product of linear NGR is characterized by loss of 17 Da. Remarkably, in both cases the kinetics of peptide degradation markedly depend on buffer composition and temperature.

Regarding the chemical structures of the degradation products, we have previously shown that cyclic NGR can deamidate and generate a 1:3 mixture of DGR and *iso*DGR, with a gain of 1 Da (42). This reaction can likely account also for the gain of 1 Da observed with the peptides analyzed in this study. The chemical structure of the main degradation product of linear NGR, *i.e.* the −17 Da molecular species, is less obvious. It is unlikely that this product corresponds to succinimide intermediate of deamidation reaction, as it was stable (by mass spectrometry analysis) even after long incubation times. Because peptides containing Asn in second position may undergo additional intramolecular reactions involving the N-terminal α-amino group, with loss of ammonia (17 Da) and formation of a seven-membered ring (41), we hypothesize that the −17 Da molecular species correspond to this product. Alternatively, the α-amino group of the succinimide intermediate can react with the succinimide ring forming a six-membered ring (diketopiperazine, DKP) (40). These reactions are not mutually exclusive and given that both DKP and seven-ring membered compound are characterized by the same molecular mass, it is likely that the −17 Da product is a mixture of both, although in an unknown proportion. This hypothesis is strongly supported by the observation that acetylation of the α-amino group of GNGRG completely prevented the formation of the −17 Da degradation products. A schematic representation of the proposed degradation reactions of CNGRC and GNGRG peptides is shown in Fig. 4. The different degradation patterns of cyclic and linear peptides can be explained by the fact that the disulfide bridge reduces peptide bond flexibility and, consequently, decreases the potential reactivity of the α-amino group with the Asn side chain or with the succinimide intermediate.

Regarding the functional properties of NGR peptide degradation products, we have previously shown that *iso*DGR, but not DGR, can bind $\alpha v\beta3$ integrin (33). Remarkably, the results of $\alpha v\beta3$ integrin-binding studies showed that the +1 Da product (*i.e. iso*DGR/DGR), but not the −17 Da product, is capable to bind this integrin. This observation can be explained by the results of previous NMR studies of *iso*DGR peptides, and of $\alpha v\beta3$-docking experiments, showing that the side chain and the negative charge of isoaspartate are critically involved in the interaction with the RGD-binding pocket of $\alpha v\beta3$ (35).

Overall, these results highlight the crucial role of flanking residues and molecular constraints for the biochemical and biological properties of the NGR motif, with important implications for the design of NGR-drug conjugates and fusion proteins. Indeed, the biological properties of drugs prepared with different NGR peptide scaffolds could be different, either

FIGURE 4. **Schematic representation of potential cyclic and linear NGR peptide degradation reactions.** *A*, nucleophilic attack of the backbone NH center (*blue*) on the Asn side chain (*red*) of cyclic CNGRC leads to formation of a succinimide intermediate (−17 Da), which after hydrolysis may lead to formation of Asp and *iso*Asp (+1 Da). *B*, succinimide formation and hydrolysis can occur also with linear GNGRG. However in this case, the succinimide intermediate may also react with α-amino group leading to the formation of seven-membered ring or diketopiperazine (*DKP*).

because of different affinity for CD13-positive endothelial cells, or because of differential degradation reactions, particularly those involving the generation of *iso*DGR, that may occur during drug preparation and storage.

The structure of peptide scaffold is crucial not only for favoring or unfavoring certain degradation reactions of NGR, but also for the receptor binding affinity and specificity of *iso*DGR, a motif that besides representing an important NGR degradation products is also an efficient ligand for targeted delivery of drugs and particles to $\alpha v\beta 3$-positive tumor neovasculature (36). In particular, we observed that *iso*DGR peptides can bind, besides $\alpha v\beta 3$, other integrins, such as $\alpha v\beta 5$, $\alpha v\beta 6$, $\alpha v\beta 8$, and $\alpha 5\beta 1$, but not $\alpha 1\beta 1$, $\alpha 3\beta 1$, $\alpha 4\beta 7$ $\alpha 6\beta 4$, or $\alpha 9\beta 1$. Remarkably, binding affinity and specificity strongly depended on flanking residues. For instance, while non-acetylated cyclic *iso*DGR (*iso*DGR-2C) could bind $\alpha v\beta 3$ with an affinity 10–100-fold greater than $\alpha v\beta 5$, $\alpha v\beta 6$, $\alpha v\beta 8$, and $\alpha 5\beta 1$, the acetylated peptide (*ac-iso*DGR-2C) bound $\alpha v\beta 3$, $\alpha v\beta 6$, and $\alpha 5\beta 1$ with similar affinities. Furthermore, peptide linearization was associated with 100-fold loss of $\alpha v\beta 3$ binding affinity and loss of specificity. Accordingly, linear peptides were less potent in inhibiting endothelial cell adhesion and tumor growth than cyclic peptides.

These findings support the concept that the molecular scaffold is very critical also for the biological properties of *iso*DGR peptides, with important implications for the design of *iso*DGR-drug conjugates and for the potential function of different *iso*DGR sites in natural proteins. Indeed, we have previously shown that spontaneous transition of NGR to *iso*DGR can occur in fibronectin, an extracellular matrix (ECM) protein that contains four NGR sites flanked by different residues (including GNGRG), generating new αv-integrin binding sites (33). Using genetically modified mice, other investigators have demonstrated that *iso*DGR can play an important role in fibronectin fibril formation (37). The finding that G*iso*DGRG and C*iso*DGRC peptides can bind integrins with different affinity may suggest that the various NGR sites in fibronectin can generate integrin binding sites with differential properties depending on flanking residues and molecular microenvironment.

In conclusion, a growing body of evidence suggests that the NGR and *iso*DGR motives are important tools for developing drugs and imaging agents that target the tumor neovasculature, and that these motives can play a physiological role in ECM proteins. Our results, showing that the molecular scaffolds markedly affect peptide stability and receptor binding specificity could provide important information for drug design, production, stabilization, development, and mechanism of action, and can stimulate further work to investigate the role of different NGR sites in fibronectin and other ECM proteins.

REFERENCES

1. Arap, W., Pasqualini, R., and Ruoslahti, E. (1998) *Science* **279,** 377–380
2. Pasqualini, R., Koivunen, E., Kain, R., Lahdenranta, J., Sakamoto, M., Stryhn, A., Ashmun, R. A., Shapiro, L. H., Arap, W., and Ruoslahti, E. (2000) *Cancer Res.* **60,** 722–727
3. Curnis, F., Arrigoni, G., Sacchi, A., Fischetti, L., Arap, W., Pasqualini, R., and Corti, A. (2002) *Cancer Res.* **62,** 867–874
4. Corti, A., Curnis, F., Arap, W., and Pasqualini, R. (2008) *Blood* **112,** 2628–2635
5. Curnis, F., Sacchi, A., Borgna, L., Magni, F., Gasparri, A., and Corti, A. (2000) *Nat. Biotechnol.* **18,** 1185–1190
6. Colombo, G., Curnis, F., De Mori, G. M., Gasparri, A., Longoni, C., Sacchi, A., Longhi, R., and Corti, A. (2002) *J. Biol. Chem.* **277,** 47891–47897
7. Curnis, F., Sacchi, A., and Corti, A. (2002) *J. Clin. Invest.* **110,** 475–482
8. Curnis, F., Gasparri, A., Sacchi, A., Cattaneo, A., Magni, F., and Corti, A. (2005) *Cancer Res.* **65,** 2906–2913
9. Sacchi, A., Gasparri, A., Curnis, F., Bellone, M., and Corti, A. (2004) *Cancer Res.* **64,** 7150–7155
10. Gasparri, A. M., Jachetti, E., Colombo, B., Sacchi, A., Curnis, F., Rizzardi, G. P., Traversari, C., Bellone, M., and Corti, A. (2008) *Mol. Cancer Ther.* **7,** 3859–3866
11. Pastorino, F., Brignole, C., Marimpietri, D., Cilli, M., Gambini, C., Ribatti, D., Longhi, R., Allen, T. M., Corti, A., and Ponzoni, M. (2003) *Cancer Res.* **63,** 7400–7409
12. Pastorino, F., Brignole, C., Di Paolo, D., Nico, B., Pezzolo, A., Marimpietri, D., Pagnan, G., Piccardi, F., Cilli, M., Longhi, R., Ribatti, D., Corti, A., Allen, T. M., and Ponzoni, M. (2006) *Cancer Res.* **66,** 10073–10082
13. Citterio, G., Santoro, A., Pressiani, T., Scalamogna, R., Gregorc, V., Rossoni, G., Donadoni, G., Caligaris-Cappio, F., Lambiase, A., and Bordignon, C. (2008) *Ann Oncol.* **19,** viii178
14. Rimassa, L., Sobrero, A., Santoro, A., Andretta, V., Gregorc, V., Sclafani, F., Caprioni, F., Caligaris-Cappio, F., Lambiase, A., and Bordignon, C. (2008) *Ann. Oncol.* **19,** viii136
15. Ceresoli, G., Gregorc, V., Zucali, P., Noberasco, C., Bajetta, E., Santoro, A., Viganò, M., Caligaris-Cappio, F., Lambiase, A., and Bordignon, C. (2008) *Ann. Oncol.* **19,** viii119
16. Ellerby, H. M., Arap, W., Ellerby, L. M., Kain, R., Andrusiak, R., Rio, G. D., Krajewski, S., Lombardo, C. R., Rao, R., Ruoslahti, E., Bredesen, D. E., and Pasqualini, R. (1999) *Nat. Med.* **5,** 1032–1038
17. Meng, J., Yan, Z., Wu, J., Li, L., Xue, X., Li, M., Li, W., Hao, Q., Wan, Y., Qin, X., Zhang, C., You, Y., Han, W., and Zhang, Y. (2007) *Cytotherapy* **9,** 60–68
18. Meng, J., Ma, N., Yan, Z., Han, W., and Zhang, Y. (2006) *J. Biochem.* **140,** 299–304
19. von Wallbrunn, A., Waldeck, J., Höltke, C., Zühlsdorf, M., Mesters, R., Heindel, W., Schäfers, M., and Bremer, C. (2008) *J. Biomed. Opt.* **13,** 011007
20. Yokoyama, Y., and Ramakrishnan, S. (2005) *Cancer* **104,** 321–331
21. Buehler, A., van Zandvoort, M. A., Stelt, B. J., Hackeng, T. M., Schrans-Stassen, B. H., Bennaghmouch, A., Hofstra, L., Cleutjens, J. P., Duijvestijn, A., Smeets, M. B., de Kleijn, D. P., Post, M. J., and de Muinck, E. D. (2006) *Arterioscler. Thromb. Vasc. Biol.* **26,** 2681–2687
22. Zarovni, N., Monaco, L., and Corti, A. (2004) *Hum. Gene Ther.* **15,** 373–382
23. Grifman, M., Trepel, M., Speece, P., Gilbert, L. B., Arap, W., Pasqualini, R., and Weitzman, M. D. (2001) *Mol. Ther.* **3,** 964–975
24. Liu, L., Anderson, W. F., Beart, R. W., Gordon, E. M., and Hall, F. L. (2000) *J. Virol.* **74,** 5320–5328
25. Moffatt, S., Wiehle, S., and Cristiano, R. J. (2005) *Hum. Gene Ther.* **16,** 57–67
26. Moffatt, S., and Cristiano, R. J. (2006) *Int. J. Pharm.* **321,** 143–154
27. Holle, L., Song, W., Hicks, L., Holle, E., Holmes, L., Wei, Y., Li, J., Wagner, T., and Yu, X. (2004) *Oncol. Rep.* **11,** 613–616
28. Zhang, Z., Harada, H., Tanabe, K., Hatta, H., Hiraoka, M., and Nishimoto, S. (2005) *Peptides* **26,** 2182–2187
29. Dirksen, A., Langereis, S., de Waal, B. F., van Genderen, M. H., Meijer, E. W., de Lussanet, Q. G., and Hackeng, T. M. (2004) *Org. Lett.* **6,** 4857–4860
30. Oostendorp, M., Douma, K., Hackeng, T. M., Dirksen, A., Post, M. J., van Zandvoort, M. A., and Backes, W. H. (2008) *Cancer Res.* **68,** 7676–7683
31. Majhen, D., Gabrilovac, J., Eloit, M., Richardson, J., and Ambriović-Ristov, A. (2006) *Biochem. Biophys. Res. Commun.* **348,** 278–287
32. Bieker, R., Kessler, T., Schwöppe, C., Padró, T., Persigehl, T., Bremer, C., Dreischalück, J., Kolkmeyer, A., Heindel, W., Mesters, R. M., and Berdel, W. E. (2009) *Blood* **113,** 5019–5027
33. Curnis, F., Longhi, R., Crippa, L., Cattaneo, A., Dondossola, E., Bachi, A., and Corti, A. (2006) *J. Biol. Chem.* **281,** 36466–36476

34. Geiger, T., and Clarke, S. (1987) *J. Biol. Chem.* **262,** 785–794
35. Spitaleri, A., Mari, S., Curnis, F., Traversari, C., Longhi, R., Bordignon, C., Corti, A., Rizzardi, G. P., and Musco, G. (2008) *J. Biol. Chem.* **283,** 19757–19768
36. Curnis, F., Sacchi, A., Gasparri, A., Longhi, R., Bachi, A., Doglioni, C., Bordignon, C., Traversari, C., Rizzardi, G. P., and Corti, A. (2008) *Cancer Res.* **68,** 7073–7082
37. Takahashi, S., Leiss, M., Moser, M., Ohashi, T., Kitao, T., Heckmann, D., Pfeifer, A., Kessler, H., Takagi, J., Erickson, H. P., and Fässler, R. (2007) *J. Cell Biol.* **178,** 167–178
38. Di Matteo, P., Curnis, F., Longhi, R., Colombo, G., Sacchi, A., Crippa, L., Protti, M. P., Ponzoni, M., Toma, S., and Corti, A. (2006) *Mol. Immunol.* **43,** 1509–1518
39. Gasparri, A., Moro, M., Curnis, F., Sacchi, A., Pagano, S., Veglia, F., Casorati, G., Siccardi, A. G., Dellabona, P., and Corti, A. (1999) *Cancer Res.* **59,** 2917–2923
40. Dehart, M. P., and Anderson, B. D. (2007) *J. Pharm. Sci.* **96,** 2667–2685
41. Lura, R., and Schirch, V. (1988) *Biochemistry* **27,** 7671–7677
42. Tyler-Cross, R., and Schirch, V. (1991) *J. Biol. Chem.* **266,** 22549–22556